

Supplementary Information

Functionalization of Bone Implants with Nanodiamond Particles and Angiopoietin-1 to Improve Vascularization and Bone Regeneration

Xujun Wu, Michela Bruschi, Thilo Waag, Yuan Tian, Sarah Schweeberg, Thomas Meinhardt, Robert Stigler, Karin Larsson³, Martin Funk, Doris Steinmüller-Nethl, Michael Rasse and Anke Krueger

Theoretical modelling of Ang-1 physisorption on diamond surface

In order to find the optimal surface termination of the applied ND in this study a theoretical investigation of protein adsorption on differently terminated diamond has been carried out. The chosen model, a slab of diamond, can be used for this computation as the electronic properties for nanodiamond larger than 1-2 nm are identical to those of bulk diamond.⁵¹ Additionally, it was known that the (111) and (100) planes are the most abundant and should be present on nanodiamond at least partially (exclusively for cubeoctahedral shape).⁵² Therefore, the simulation in this work was carried out with focus on the 111 and 100 diamond surface. The saturation of the dangling bonds with hydrogen (H-terminated) and oxygen containing (O-terminated) groups (adsorption of O and OH species from H₂O and O₂ in atmosphere) on-top and bridge (111) and 2x1 reconstructed (100) diamond surface have been of particular interest for investigation. A recent theoretical investigation has shown the possibility to cover a diamond (100) surface completely by using either H, O or OH.⁵³ Therefore, a 100% coverage of the various terminating species has been used in the present study.

Figure 1A shows the final optimized (O-ontop) diamond (111) surface with an adsorbed Ang-1. This molecule was first positioned in parallel with the diamond surface, and within van der Waals bonding position relative to the surface. Thereafter, the protein was allowed to be completely geometrically relaxed by performing a Molecular Dynamics annealing procedure at room temperature. The adhesion energy for the attachment of Ang-1 to diamond (111) and (100)-2x1 surfaces with different surface terminations (H, OH, O_{on-top}, and O_{bridge}) has been calculated using *ab initio* force field calculations. It can be seen in Figure 1 B that the diamond (111) surface should be more reactive towards adsorption than the diamond (100)-2x1 surface independent of the surface termination. With a few exceptions, the calculated adhesion energies are approximately twice as high for the (111) surface.

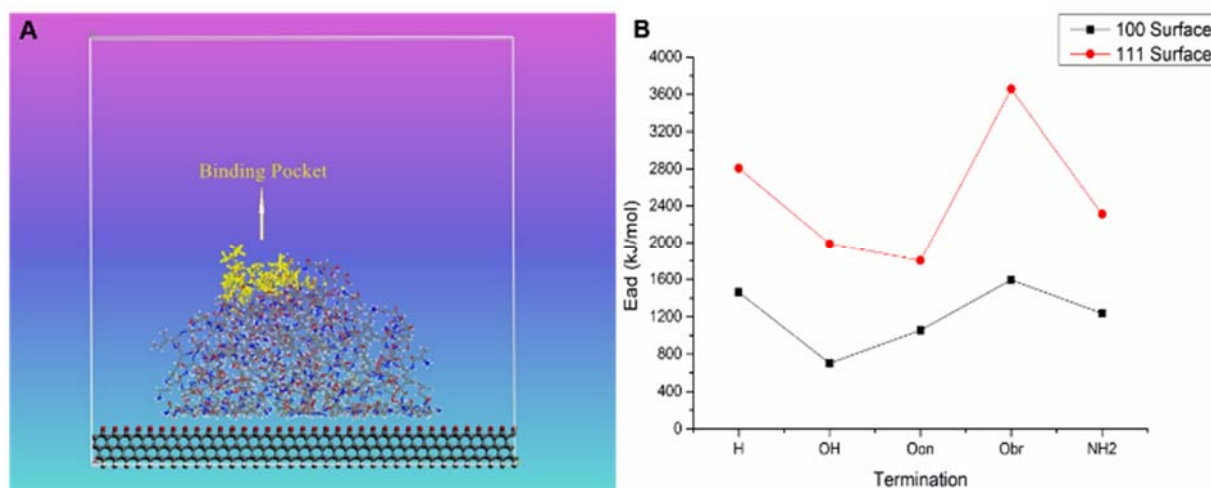


Figure S1. Computational modelling of Ang-1 attachment to ND surface. A) Final geometrical structure for Ang-1 on O-ontop diamond (111) by using *ab initio* force field COMPASS. B) Adhesion energies for Ang-1 on differently terminated diamond surfaces. Black solid line: (100)-2x1 reconstructed diamond surface, Red solid line: (111) diamond surface.

However, the order of adhesion energy differs somewhat: O_{bridge} ~ H > NH₂ > O_{on} > OH (for the 100-2x1 surface) and O_{bridge} > H > NH₂ > OH > O_{on} (for the 111 surface). Hence, it was clear that there is a preference for Ang-1 to bind to the O bridge-terminated (111) surface as compared with the (100)-2x1 surface. Moreover, for both types of surfaces there was only a small difference in adhesion energy (~ 200 kJ/mol) for O_{on}- and OH-termination.

From the theoretical investigation it is expected that ND with a mixed oxygen termination (including bridging oxygen atoms as well as OH groups and carbonyl functions) should be highly suitable for the noncovalent immobilization of Ang-1. Therefore, milled detonation nanodiamond after oxidative acid cleaning was chosen as the diamond material for this study. In the past it was shown that the surface of ND is modified during milling, the reaction of *in situ* generated dangling bonds with the solvent, i.e. water, results in a more hydrophilic surface carrying a large amount of OH groups as shown in the IR spectra.⁴³ The terminating species on ND surfaces have been shown to affect surface properties such as wettability and protein binding properties.⁵³ The ND modified scaffold should provide multiple binding sites for protein adsorption.³⁹

Zetapotential measurements before and after Ang-1 adsorption

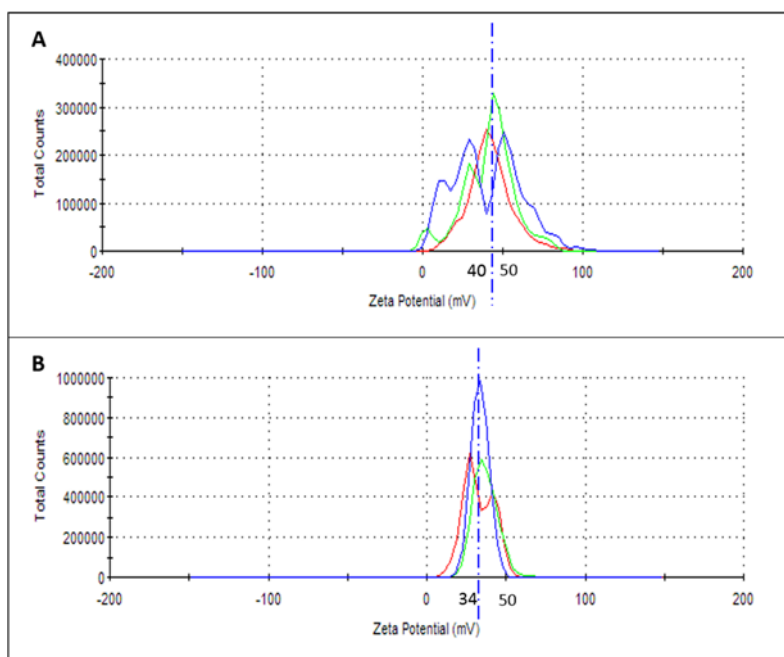
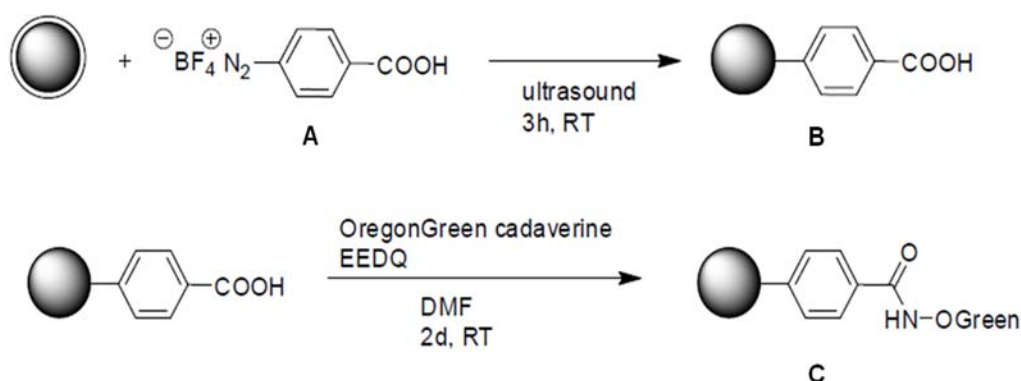


Figure S2. Zeta potential measurement of ND (A) before and (B) after Ang-1 physisorption

The zeta potential of the ND before and after physisorption of Ang-1 were +40 and +34 mV, respectively at pH = 6.

Labelling of ND with Oregon Green® 488

The general procedures for preparing the Oregon Green 488 labelled ND are shown in Scheme S1.



Scheme S1: Surface functionalization of ND using the reaction of milled detonation ND with aryl diazonium salts and the subsequent amide formation with the fluorescent dye Oregon Green® 488.

The chemical reactions for synthesis of A, B and C are as follows:

A: (4-carboxybenzenediazonium tetrafluoroborate)

2.00 g (14.6 mmol) of 4-aminobenzoic acid was suspended in 10 ml (80 mmol) of fluoroboric acid (50 wt.-% aqueous solution). After cooling to 0 °C a solution of 1.10 g (15.9 mmol) of sodium nitrite in 3 ml of water was added dropwise. The reaction mixture was stirred for 1 h and allowed to warm to room temperature. After cooling overnight the formed precipitate was filtered off. The product was washed with 20 ml cooled diethyl ether. Drying in vacuo yielded A as a colorless solid.

Yield: 2.61 g (75 %). **¹H-NMR** (400 MHz, DMSO-*d*₆): δ = 8.73 (d, ³J = 8.8 Hz, 2 H; Ar-2-*H*, Ar-6-*H*), 8.50 (d, ³J = 9.2 Hz, 2 H; Ar-3-*H*, Ar-5-*H*) ppm. **FT-IR** (ATR): $\bar{\nu}$ = 3280 (m) 3112 (m), 2297 (m), 1725 (s), 1416 (m), 1383 (m), 1312 (m), 1222 (m), 1044 (s), 974 (s), 864 (s), 761 (s) cm^{-1} .

B: (Benzoic acid functionalized beads milled ND)

0.51 g (2.1 mmol) of 4-carboxybenzenediazonium tetrafluoroborate (A) was dissolved in 2 ml of distilled H₂O and added to a 6 ml colloidal solution containing approx. 170 mg of the milled diamond nanoparticles in distilled H₂O (2.7 wt.% colloidal solution). The suspension was treated with ultrasound (Sonifier II W-450 with 5 mm microtip operated at output control = 1.5) for 3 h while cooling with a water bath. After centrifugation the nanodiamonds were washed repeatedly with water, acetone and DMF. The particles were suspended in water for further reactions.

FT-IR: $\bar{\nu}$ = 3355 (m), 2929 (m), 1702 (s), 1606 (s), 1369 (s), 1245(s), 1197 (s), 1103 (s), 860 (s) cm^{-1} . **Elemental analysis:** C: 86.04%, H: 1.61%, N: 2.32%. **Surface loading** (calculated from TGA): 0.48 mmol g^{-1} . (Δm (180 - 500 °C, fragment: C₇H₅O₂ (121.11 g mol^{-1})) **Particle size:** (H₂O; conc. 1 mg ml^{-1}): 10 % < 42 nm, 50 % < 62 nm, 90 % < 101 nm. **Zeta potential:** -44.6 mV (pH = 8.0).

C: (Oregon Green® 488 functionalized beads milled ND)

30 mg of B and 4 mg of *N*-ethoxycarbonyl-2-ethoxy-1,2-dihydroquinoline (EEDQ) (16.0 μmol) was suspended under sonication in 20 ml DMF. After stirring for one hour, 0.6 mg of Oregon Green cadaverine (1.1 μmol) was added. The reaction mixture was stirred under exclusion of light for further 18 h. After centrifugation the nanodiamonds were washed repeatedly with water and DMF.

FT-IR: $\bar{\nu}$ = 3355 (m), 2938 (m), 1705 (s), 1644 (s), 1608 (s), 1550 (m), 1500 (m), 1369 (s), 1249(s), 1176 (s), 1103 (s), 862 (s) cm^{-1} . **Particle size:** (H₂O; conc. 0.5 mg ml^{-1}): 10 % < 55 nm, 50 % < 101 nm, 90 % < 269 nm. **Zeta potential:** -32.4 mV (pH = 6.0).

Electron microscopy of ChronOS and ChronOS+ND

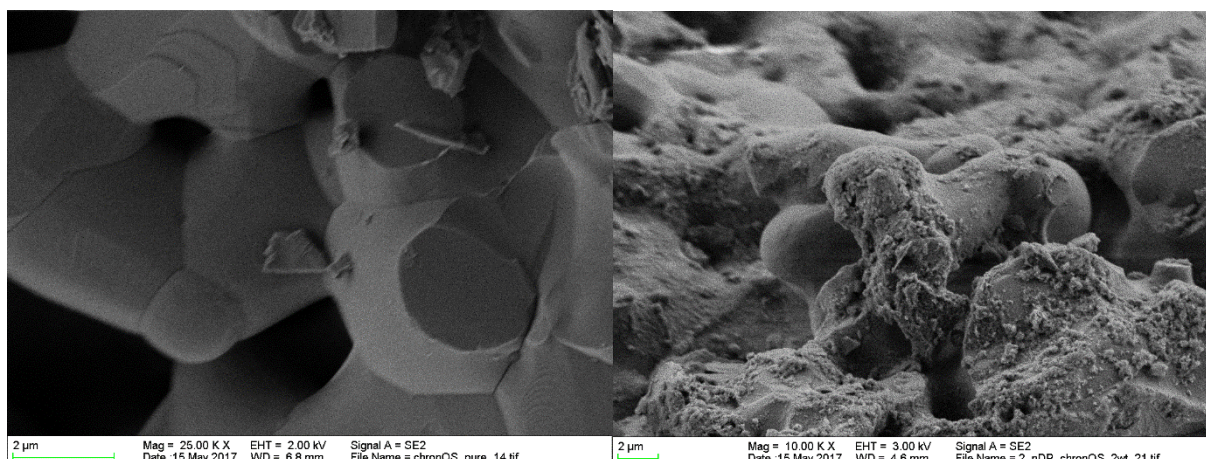


Figure S3. SEM images were taken of the bare ChronOS scaffold material (left) and the ND coated scaffold (right). As can be seen from the images the nanodiamond particles are localized at the surface of the struts of the scaffold material. Scale bar 2 μm .

Characterization of the Oregon Green[®]488 labelled ND using FTIR spectroscopy

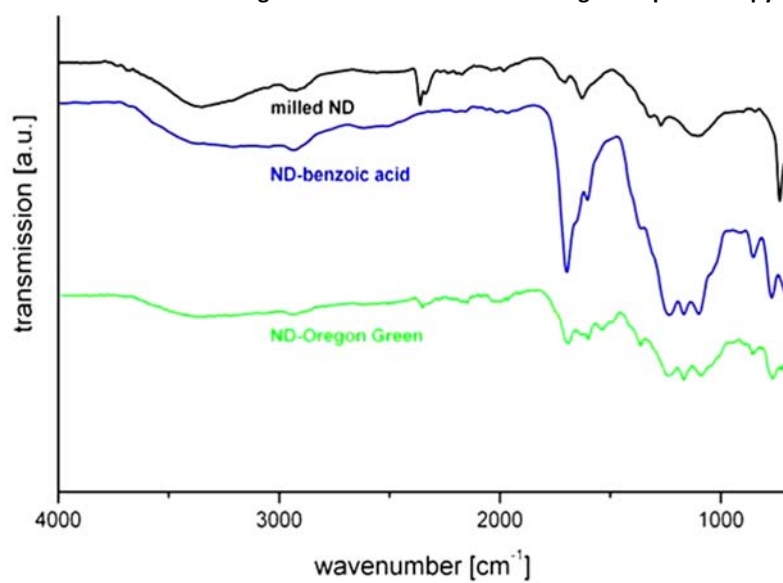


Figure S4. FTIR spectra of ND: ND after milling (black), benzoic acid functionalized beads milled ND (blue), Oregon Green[®] 488 functionalized beads milled ND (green).

Wetting behaviour of ChronOS and ChronOS+ND

Videos showing the completely different wetting behaviours of the bare β -TCP scaffold and the ChronOS+ND have been deposited on youtube.

The following links are applicable:

For bare ChronOS: <https://youtu.be/SoRiXW7pgXQ>

For ChronOS+ND: <https://youtu.be/dcQwsp9mEJk>

Pictures extracted from the video sequences are shown here for reference.



Figure S5. A water droplet deposited on bare (left) and ND treated ChronOS (right). In the case of ChronOS+ND the water droplets are immediately uptaken by the scaffold material (darker shade in the upper third of the scaffold sample).

Protein release experiments using BSA

Due to the strong interaction of proteins with nanodiamond surfaces the release of proteins from ND coated surfaces is much lower than from untreated β -TCP scaffold material. We compared the protein release from the pure and ND modified scaffolds using an Elisa microplate reader. 5 μ g of a standard protein BSA (bovine serum albumin) were diluted in 200 μ l H₂O and used for the immobilization of the protein on either the pure or the ND modified ChronOS. Scaffolds were kept in a 2ml water solution (the scaffold was kept dip in the solution inside 5ml vials) set on a shaker for 7 days at RT in a dark chamber. The washing solution was collected and replaced at different time-points (day 1,2,4,7). Protein content was measured at the ELISA microplate reader via Comassie blue[®] colorimetric assay. BSA is commonly used as test protein, due to the high cost of pure angiopoietin. In pure ChronOS 80% of the protein was released after 7 days whereas in ND modified just 4.5% of the original protein was released from the surface of the scaffold modified with nanodiamond particles.

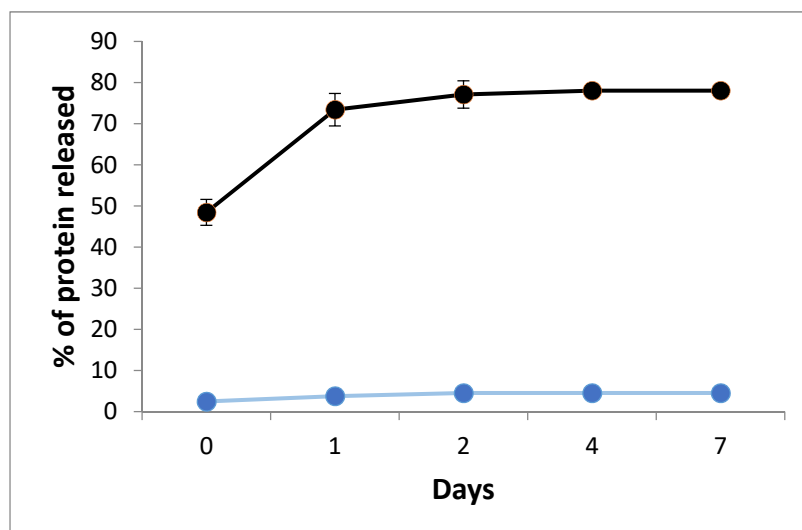


Figure S6. Protein release from ChronOS (black curve) and ChronOS+ND (blue curve) modified with 5 μ g of BSA dissolved in 200 μ L of water.

Surface area and porosity of ND coated scaffolds

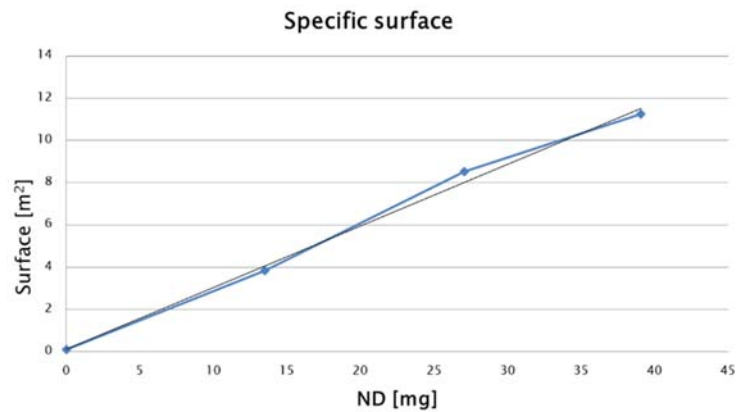


Figure S7. Surface area measurement of ND modified scaffold using BET method (blue dots) showed a linear correlation of surface area and amount of ND perfused ($y=0.2916x+0.1685$, $R^2=0.9946$).

Experimental procedures for biomedical application

In vivo implantation and evaluation:

Implantation procedures: To assess the biological responses of the ChronOS+ND with and without Ang-1, animal experiments were conducted with the approval of the national government and authorities (BMWF-66.011/0146-II/3b/2010). Briefly, 6 healthy six-year-old female sheep weighing 75 ± 5 kg were fasted overnight while having free access to water. After general anesthesia, a sagittal incision was carried out on the forehead to access the frontal bone. 10 critical size defects (1 cm diameter) with full penetration were created in each animal with a trephine burr, and special care was taken to not damage the dura mater. To prepare the ChronOS+ND+Ang-1 scaffold, PBS buffered Ang-1 (1ml, 1 μ g/ml) solution was injected in the ChronOS+ND scaffold with 1 h incubation at room temperature at a sterile condition prior to implantation. Defects were randomly filled with ChronOS, ChronOS+ND, ChronOS+ND+Ang-1 group or left unfilled as negative control. The periosteum was removed above the defects before suturing. The sheep were sacrificed after 4, 12, and 24 weeks.

Histological and immunohistochemical analysis: All explanted samples were embedded in Technovit 9100 New[®] as described previously.⁵⁴ After embedding, the hardened blocks were cut in the middle (longitudinal direction), one half was subjected to histology staining and the other half was used for immunohistochemical analysis. Sections with approx. 25 μ m thickness were stained with Toluidine Blue O for evaluation of new bone formation.⁵⁵ Sections with 10 μ m thickness were used for immunohistochemical staining according to previous reported protocols with minor modifications.⁵⁶ The samples were incubated with the mouse-anti-von Willebrand Factor (vWF) (Dako, Denmark, 1:200 dilution) overnight at 4 °C. After washing with Tris-buffered saline, samples were incubated with peroxidase-labelled secondary antibody (EnVision⁺ Dual Link System-HRP, Dako, Denmark) for 30 min at RT. Peroxidase activities were visualized with the 3-amino-9-ethylcarbazole (AEC) substrate chromogen system (Dako, Denmark). The samples were mounted with aqueous mounting medium (Aquatex, Merck, Germany) for observations.

Histomorphometry: Semi-quantitative measurements of slides with von Willebrand factor staining were performed with a Nikon NIS-elements software. The image of the whole sample was taken with Nikon Eclipse 80i microscope at 100x magnification coupled with a CCD camera using the stitching function from NIS-element software. The region of interest was defined as the area with the defect site containing tissue/scaffold reaching from periphery of the host bone. Vessels were identified as luminal structures containing erythrocytes and counted manually in a blinded manner by two independent observers. The vessel density was quantified using the number of positively stained vessels divided by the total area of interest, which was then presented as number of vessels per area (vessels/mm²).

Statistical analysis: Statistical evaluation was performed using the Kruskal–Wallis tests with Graphpad Prism software package. $P < 0.05$ is considered as significant differences between the groups.

Bone healing of empty defect 24 weeks post-operation

Within the empty defect, minimal bone formation at the periphery and dense fibrous tissue in the centre of the defect were observed.

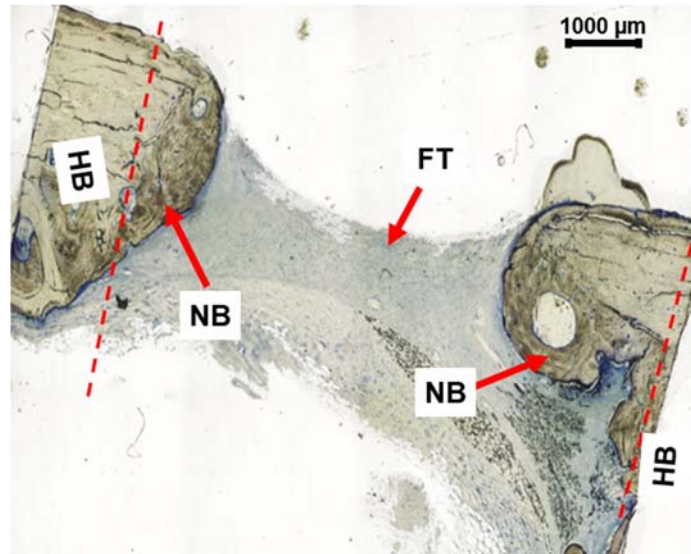


Figure S8. Histology of the empty defect without bone implant 24 weeks post-operation. Dotted lines represent edges of the original defect. Longitudinal sections stained with Toluidine Blue O. (NB = new bone, HB = host bone, FT = fibrous tissue).

Specifications of clinically approved ChronOS β -TCP scaffold material

The supplier (SYNTHES®) data sheet for chronOS® “Synthetic cancellous bone graft substitute (β -tricalcium phosphate)” can be found under the following link: https://orto.hi.is/skrar/305_chronos_english220.pdf

The main specifications according to the data sheet are as follows:

- Replaced by bone in 6-18 months
- Compressive strength 7.5 +/- 1 MPa
- Total porosity 70 % for blocks, wedges and cylinders
- Interconnected macropores in the range of 100-500 μ m
- Micropores smaller than 10 μ m

TEM images of the applied detonation nanodiamond

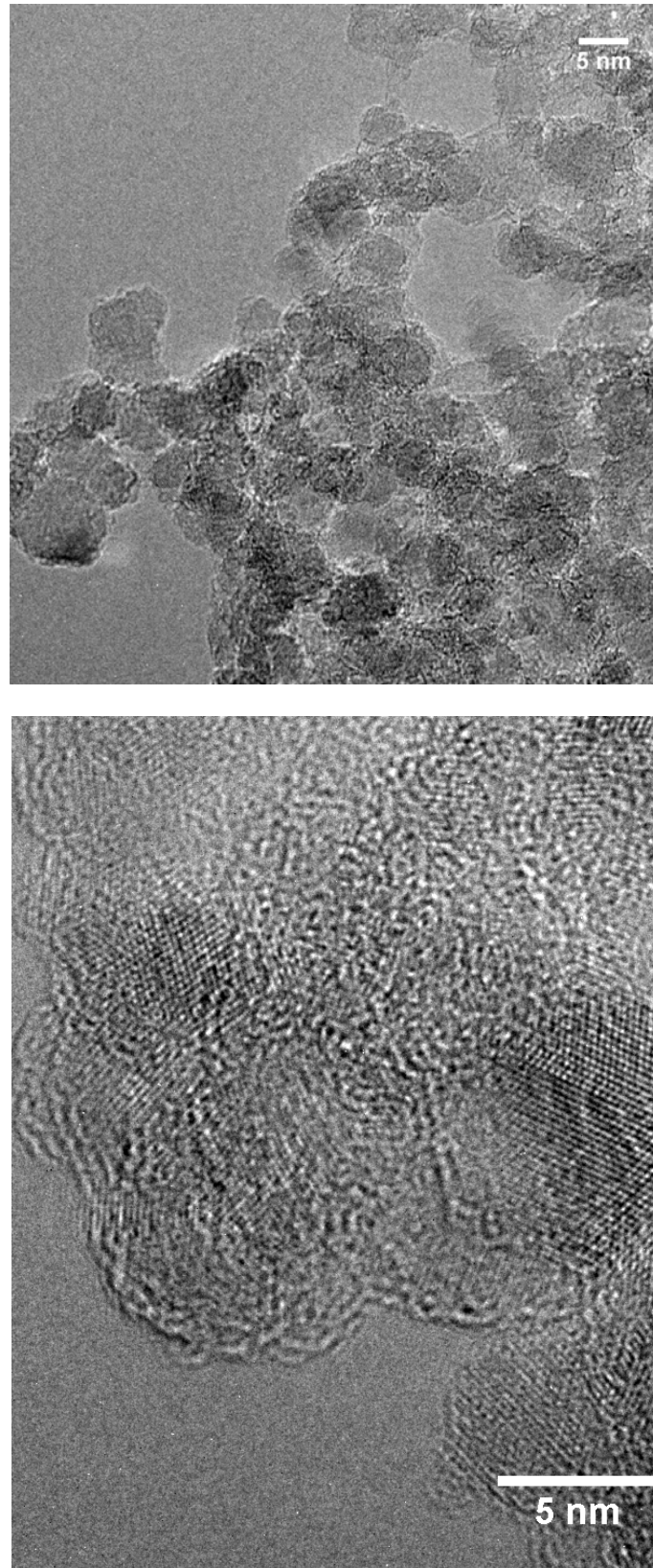


Figure S9. HRTEM images of the applied detonation nanodiamond at different magnifications top: overview, bottom: magnification showing the diamond lattice planes). As can be seen from the micrographs the diamond nanoparticles exhibit a roundish morphology without pronounced facets and edges. The particles are clustered due to the TEM sample preparation by dropcasting followed by drying the sample grid. Scale bars 5 nm.

Supplementary references:

- S1 Y. Tian and, K. Larsson, *J. Phys. Chem C.*, 2015, **119**, 8608-8618.
S2 L. Lai and A. S. Barnard, *RSC Adv.*, 2012, **4**, 1130-1137.
S3 D. Petrini and K. Larsson, *J. Phys. Chem. C*, 2007, **111**, 795-801.
S2 R. Yang, C. M. Davies, C. W. Archer and R. G. Richards, *Eur. Cells Mater.*, 2003, **6**, 57-71.
S3 K. Donath and G. A Breuner, *J. Oral Pathol.*, 1982, **11**, 318-326.
S4 P. Rippstein, M. K. Black, M. Boivin, J. P. Veinot, X. L. Ma, Y. X. Chen, P. Human, P. Zilla and E. R. O'Brien, *J. Histochem. Cytochem.*, 2006, **54**, 673-681.

Author contributions

A. Krueger, M. Rasse, D. Steinmüller-Nethl and K. Larsson designed the research project

A. Krueger and X. Wu wrote the manuscript

T. Waag, S. Schweeberg, T. Meinhardt synthesized and characterized the nanodiamond materials

D. Steinmüller-Nethl and M. Funk produced the coated scaffold materials and characterized the modified scaffolds.

Y. Tian and K. Larsson carried out the computational calculations.

X. Wu, M. Bruschi, R. Stigler and M. Rasse carried out the animal study.

All authors contributed to the discussion of the results and commented on the manuscript. There is no conflict of interest for any of the authors.